J Appl Physiol
90: 1639–1647, 2001.

Effect of combined recompression and air, oxygen, or heliox breathing on air bubbles in rat tissues

O. HYLDEGAARD,[1] D. KEREM,[2] AND Y. MELAMED[2]
[2]*The Israeli Naval Hyperbaric Institute, Haifa 31080, Israel; and* [1]*The Institute of Medical Physiology, The Panum Institute, University of Copenhagen, 2200-N Copenhagen, Denmark*

Received 10 June 1999; accepted in final form 27 November 2000

Hyldegaard, O., D. Kerem, and Y. Melamed. Effect of combined recompression and air, oxygen, or heliox breathing on air bubbles in rat tissues. *J Appl Physiol* 90: 1639–1647, 2001.—The fate of bubbles formed in tissues during the ascent from a real or simulated air dive and subjected to therapeutic recompression has only been indirectly inferred from theoretical modeling and clinical observations. We visually followed the resolution of micro air bubbles injected into adipose tissue, spinal white matter, muscle, and tendon of anesthetized rats recompressed to and held at 284 kPa while rats breathed air, oxygen, heliox 80:20, or heliox 50:50. The rats underwent a prolonged hyperbaric air exposure before bubble injection and recompression. In all tissues, bubbles disappeared faster during breathing of oxygen or heliox mixtures than during air breathing. In some of the experiments, oxygen breathing caused a transient growth of the bubbles. In spinal white matter, heliox 50:50 or oxygen breathing resulted in significantly faster bubble resolution than did heliox 80:20 breathing. In conclusion, air bubbles in lipid and aqueous tissues shrink and disappear faster during recompression during breathing of heliox mixtures or oxygen compared with air breathing. The clinical implication of these findings might be that heliox 50:50 is the mixture of choice for the treatment of decompression sickness.

decompression sickness; treatment; perfusion; diffusion; countercurrent

CONVENTIONAL TREATMENT OF decompression sickness consists of recompression combined with oxygen breathing (11). The purpose is to *1*) reduce bubble size by compression of the gas phase, *2*) maximize inert gas partial pressure gradients from bubbles and tissues to the blood, and *3*) improve oxygenation of stricken tissues (45). The first goal is achieved solely by recompression, regardless of the breathing mixture used, whereas oxygen breathing would best achieve the latter two goals. However, using a breathing mixture with an inert gas different from that present in the bubble (nitrogen when considering air dives) may also be advantageous, provided that the new gas will enter the bubble at a slower rate than nitrogen leaves it.

On the basis of the suggestions of James (26), which were theoretically supported by Hills (13), the Companie Maritime d'Expertises (Comex) Medical Book was revised in 1986, from then on recommending heliox 50:50 instead of nitrox 50:50 as the therapeutic breathing mixture in the Cx_{30} table (27). This concept has since gained increasing clinical usage in the treatment of both commercial and amateur divers. Helium is less soluble in blood as well as in lipid and aqueous tissues and is more diffusive in aqueous tissue but has a lower partition coefficient than nitrogen between lipid tissues and blood (46). The actual counter fluxes of nitrogen and helium across the boundaries of the bubble-tissue-blood complex are, however, hard to predict. The few attempted model simulations (15, 42), direct observations of bubbles in gelatin (38), and experimental pulmonary embolization (35) all point to bubble growth in some (aqueous) tissues during heliox breathing. On the other hand, considerable clinical evidence documents the effectiveness of heliox treatment tables for air-dive-induced neurological decompression sickness (7, 8, 10, 12, 16, 25, 29, 36). The beneficial effects of heliox 80:20 (i.e., 80% helium in 20% oxygen) breathing are in accordance with experimental observations previously reported by Hyldegaard and colleagues (19, 20, 23, 24), in which decompression-induced or injected micro-bubbles were studied in lipid and aqueous tissues at 101.3 kPa.

The effects of changes in breathing gas at higher pressures may differ from those observed at sea level. Visual examination of bubble size changes under these conditions has, to our knowledge, not previously been reported; therefore, we decided to extend previous experiments (19, 20, 23, 24) at 101.3 kPa on decompressed rats, in which bubble kinetics in vivo were followed by direct visualization while the animals breathed various gas mixtures. Hyldegaard et al. showed that bubbles appearing in rat adipose tissue, as well as air bubbles injected into spinal white matter, muscle, or tendon, will grow for hours during air breathing but shrink and disappear during breathing of heliox 80:20. During oxygen breathing, some bubbles grew initially up to two- to threefold (i.e., in adipose tissue and spinal white matter) before shrinking and disappearing in approximately the same time as during heliox breathing. Similarly, both heliox 80:20 and

Address for reprint requests and other correspondence: O. Hyldegaard, Dept. of Medical Physiology, The Panum Institute, Blegdamsvej 3c, 2200 Copenhagen N., DK-Denmark (E-mail: ole.hyldegaard@dadlnet.dk).

The costs of publication of this article were defrayed in part by the payment of page charges. The article must therefore be hereby marked "*advertisement*" in accordance with 18 U.S.C. Section 1734 solely to indicate this fact.

oxygen breathing at 101.3 kPa abate the deterioration in spinal conductive function, as judged by spinal-evoked potentials, after decompression from a hyperbaric air exposure. The effect of heliox 80:20 appeared to be superior to that of oxygen breathing (24).

The purpose of the present experiments was to examine the combined effects of recompression and air, heliox 80:20, heliox 50:50, or oxygen breathing on the size of air bubbles injected into lipid and aqueous tissues of rats decompressed from a prolonged air exposure. Recompression pressures of 284 kPa and 405 kPa for the heliox 50:50 mixture (Comex CX_{30} treatment table) were used.

METHODS

Animal Preparation and Experimental Protocol

Female Wistar rats weighing 250–350 g were anesthetized with sodium thiomebumal (0.1 g/kg) intraperitoneally. The rat was placed supine on the operating table, and a cannula was inserted into the trachea (i.e., polyethylene tubing, 1.5 mm ID). A catheter was placed in the left carotid artery for blood pressure registration. It was kept patent by continuous infusion of saline (1 ml/h) (SAGE Instruments, syringe pump model 341). Mean arterial blood pressure (MAP) was measured by use of a Statham AA pressure transducer, and body temperature was measured by a thermocouple (Yellowstone) placed in the vagina. A continuous record was obtained on a Gould 2600 multichannel recorder. In some of the experiments, a thermoprobe was placed superficially on the tissue to measure the temperature at the surface of the exposed tissue.

All experimental groups of animals were subjected to two pressure exposures; the first compression was breathing air to induce a state of nitrogen supersaturation. In experiments on spinal white matter, muscle, and tendon, the initial hyperbaric exposure was 1 h at 355 kPa followed by a 7.5-min decompression with short pauses at 324 and 152 kPa (18, 20). In experiments on adipose tissue, the initial exposure was 4 h at 314 kPa followed by a 20-min decompression in three stages (23). After decompression from the initial hyperbaric exposure, the animals were placed under a heating lamp and allowed to breathe air at 101.3 kPa. One to three air bubbles of 0.5–2.0 μl were injected with a micropipette into the specified tissue (adipose 1.5–2.0 μl, spinal white matter 1.0–1.5 μl, muscle 1.0–1.5 μl, or tendon 0.5–1.0 μl, according to the designated experimental group; for further details see Refs. 23 and 20). The duration of this interval was 20–70 min, depending on the tissue studied. During this period, body temperature was maintained by a heating lamp. The rat was replaced in the chamber, the lid was resealed, and the microscope was focused on a bubble for determination of the prerecompression bubble size. Subsequently, the animal was switched to the specified breathing gas and recompressed at 101.3 kPa/min to 284 kPa or to 405 kPa in some spinal white matter heliox 50:50 trials. The second bubble-size measurement, reflecting bulk compression, was then obtained, and subsequently the bubbles were monitored continuously until their total disappearance. After disappearance of the bubble, decompression followed immediately at 101.3 kPa/min with continuous inspection for reappearance of the bubble. The chamber temperature was regulated at 28–29°C to maintain a body temperature of 37°C.

After the final decompression, the thorax and abdomen were opened for further microscopic examination for intra- or extravascular gas formation, whereupon the animal was killed by exsanguination.

Pressurization System

Compression and decompression were performed in a specially designed vertical pressure chamber with a horizontal viewing port in the lid. The animal was strapped supine on a circular plate that could be lifted out of the chamber and serve as an operating platform. The plate had a mounting for a stereotactic head-holding device, which was used in the spinal cord experiments in which the rat was in the prone position. When inside the chamber, the plate was positioned such that the tissue under observation was placed 2 cm below the glass window (Fig. 1).

The chamber was compressed on air through an inlet fitted with a regulator (AR 425, Baccara) that maintained the desired chamber pressure. The chamber had penetrations for a copper spiral water-heating coil, infusion pump, pressure transducer, temperature sensors, and electric cables, as well as breathing gas supply and exhaust. The breathing mixture entered at a pressure slightly above chamber pressure and passed a T connection for the animal's tracheal tube before escaping to the outside via a modified Ultralite mask (Orthomed) overboard dump valve. The valve was adjusted to maintain a 2 cmH_2O positive pressure inside the loop. The breathing gas flow was 1,500–2,000 ml/min, as verified by a Krohn 90044D flowmeter attached to the outlet port outside the chamber.

Bubble Monitoring System

Bubbles were observed through the chamber window at ×40 magnification by means of a Wild M10 stereo microscope with a long focal-length objective. The bubble field was illuminated by two flexible fiber optic light guides attached to a Volpo Intralux 5000 lamp. A Kappa CF 15/2 color video camera was fitted to the microscope, and the field was both displayed on a TV screen and recorded on VHS videotape (Fig. 1). With a frame grabber board, real-time images could be grabbed to a Macintosh IISi computer. The bubble's apparent cross-sectional area on the microscopic image could be computed at any time by hand tracing its circumference (often irregular) and applying an IMAGE version 1.61 automated planimetry program (33). The computer program was calibrated by placing a metal rod, 200 μm in diameter, on top of the exposed tissue and within the microscopic picture.

Data Analysis and Statistics

Except for some transient changes to be described below, the curve describing visible area vs. time did not differ from a linear function. Therefore, bubble shrinking rates were expressed as the slope of the line (in μm^2/min) from the first observation after recompression to 284 kPa (or 405 kPa) and to the disappearance of the bubble. Group mean ± SD values of bubble shrinking rates are given. When several bubbles were studied in one animal, their average value was recorded. Analysis of variance (ANOVA) was used to assess whether the differences between group mean values of calculated bubble shrinking rates were different from zero (3, 37). The differences between mean values of the various treatment groups were then analyzed by use of the Student-Newman-Keuls procedure for multiple comparison of means between groups (3, 37). $P < 0.05$ is regarded as the limit for significance.

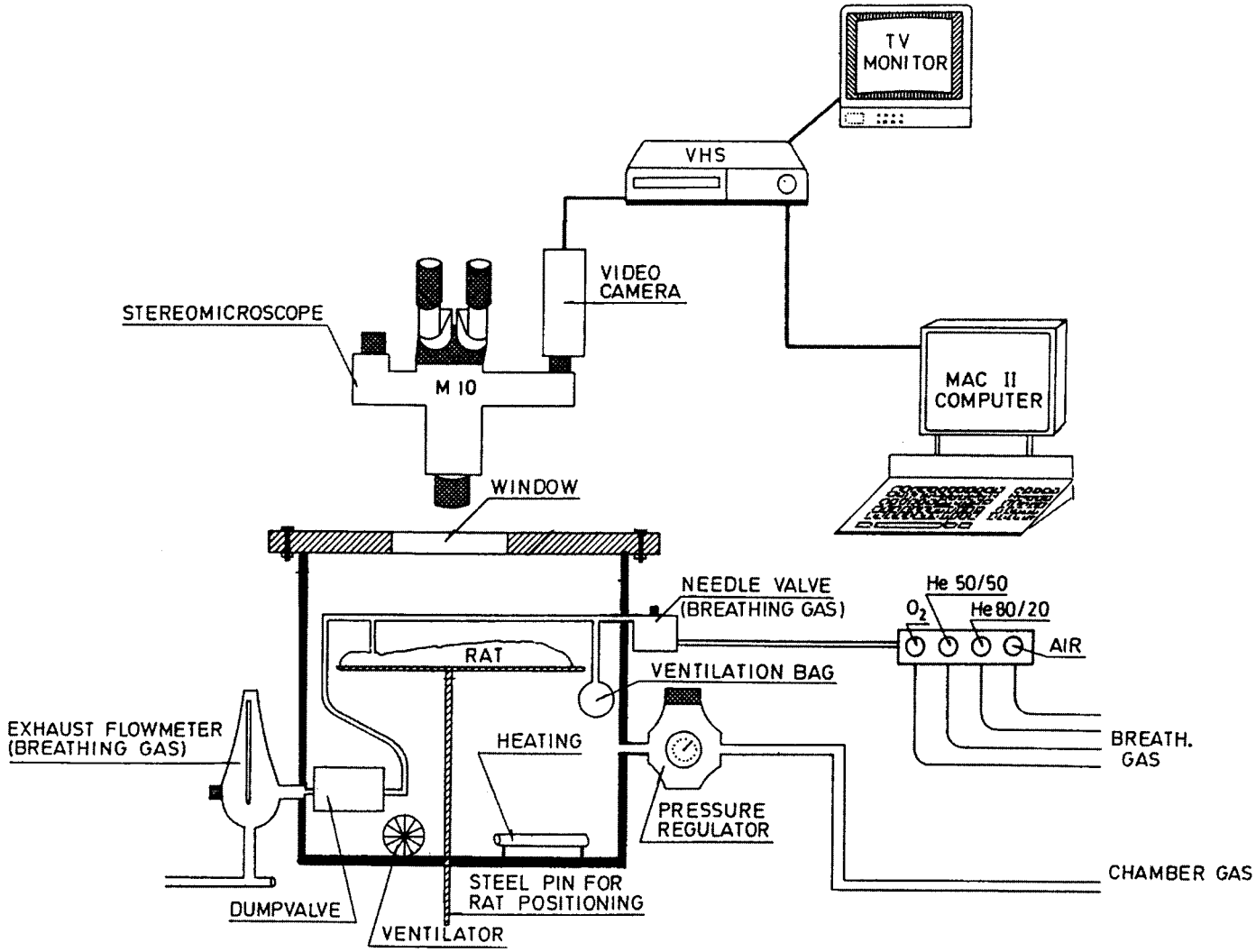

Fig. 1. Experimental setup with pressure chamber, connections, and respiratory system. The stereo microscope is a Leica model Wild M10. He 50/50, heliox 50:50 breathing mixture; He 80/20, heliox 80:20 breathing mixture.

RESULTS

Effects of Compression on Bubbles

Figures 2–5 illustrate the primary data with oxygen as the breathing gas, demonstrating transient bubble growth, which is not seen during breathing of air or heliox mixtures. Accordingly, only the oxygen curves are shown.

In general, the observed cross-sectional area of all bubbles was reduced in proportion to the initial recompression. In adipose tissue (see Fig. 2), in which most bubbles were spherical, the Boyle-Mariotte effect of an increase in pressure from 101.3 to 284 kPa should reduce the bubble area by a factor $2.8^{-2/3} = 0.503$ provided that the same cross-sectional area of the bubble is seen before and after pressurization. In Fig. 2, the area reduction from *point 1* to *point 2* is of this magnitude or somewhat larger, which may reflect nitrogen absorption under the increased pressure and/or an increased effect of surface tension in the smaller bubble. The effect of the initial recompression is represented by the steep line between the first two observation points at the curves (Figs. 2–5). The fate of the bubble from then on depended on the breathing gas (see below). No bubbles reappeared during the decompression, which was initiated within 1 min after the disappearance of the bubble from view. Mean values for shrinking rates in recompressed animals are given in Table 1 and Fig. 6. Rates of decline of cross-sectional area were linear throughout.

Effects of Breathing Gases on Recompressed Bubbles

Bubble shrinking rates for all the breathing gases used are given in Table 1 and graphed in Fig. 6. During air breathing, all bubbles shrank until they disappeared. Similarly, heliox 80:20 and heliox 50:50 breathing caused bubbles to shrink consistently until they disappeared.

Oxygen breathing caused all bubbles to shrink and disappear (Table 1). However, in adipose tissue (Fig. 2), four bubbles were observed to grow for 5–20 min at pressure (i.e., 284 kPa). Subsequently, they shrank and disappeared at a rate faster than during air

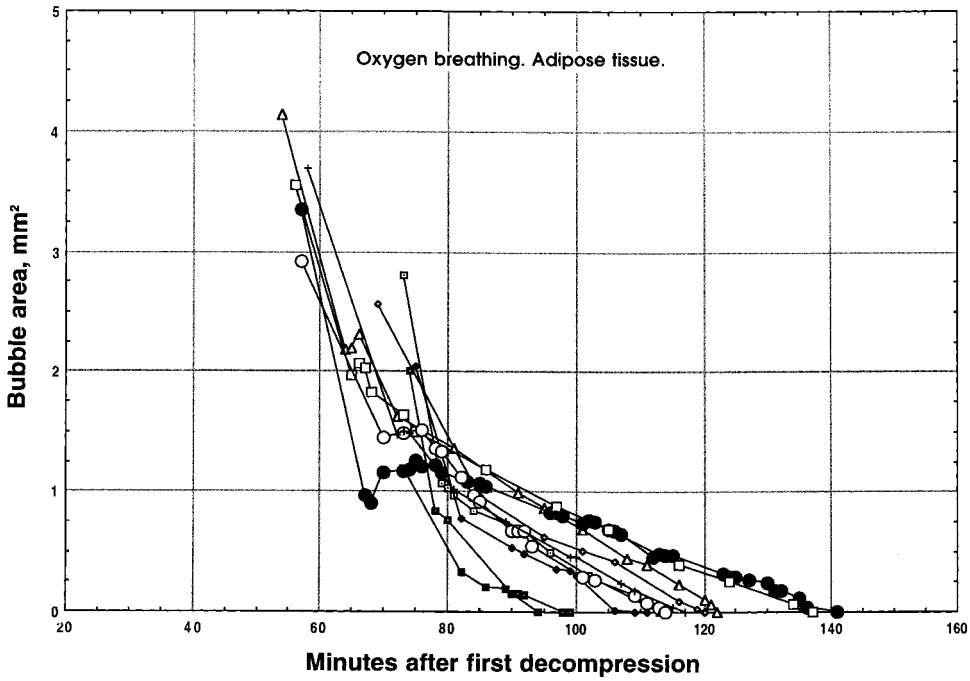

Fig. 2. Effect of combined recompression and oxygen breathing on air bubbles in rat adipose tissue. Recompression was to 284 kPa between first and second point of each curve. Bubble shrinking rate was recalculated from μm^2/min to mm^2/min. Individual symbols represent 1 bubble curve.

breathing. One bubble in adipose tissue grew 1.39-fold in area, corresponding to a 1.64-fold increase in volume. In spinal white matter (Fig. 3), oxygen breathing at pressure caused 5 of 6 bubbles to grow transiently for ~4–7 min, from which point they all started shrinking until they disappeared from view. One bubble in spinal white matter grew 1.16-fold before shrinking and disappearing (Fig. 3). In muscle (Fig. 4), 1 bubble out of 10 grew transiently for a short period of 5–6 min before it started to shrink. It was noted that perfusion of the immediate bubble surroundings was sluggish. During oxygen breathing in tendon, 5 of 11 bubbles grew or stopped shrinking for a period of 5–15 min, after which they began to shrink until they disappeared (Fig. 5). One bubble in tendon grew 1.21-fold before shrinking (Fig. 5). Such transient growth of bubbles was not observed during breathing of either heliox 80:20 or heliox 50:50. In spinal white matter, bubbles shrank consistently at a rate of $22.3 \times 10^3 \pm 7.5 \times 10^3$ μm^2/min during heliox 50:50 breathing with recompression to 405 kPa (i.e., the Comex CX_{30} treatment table).

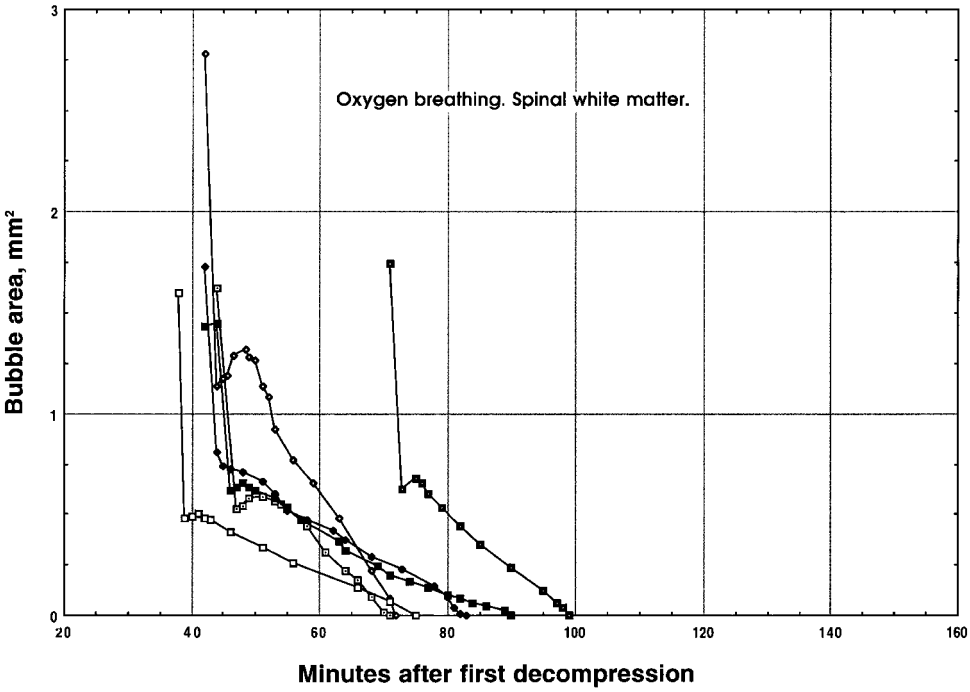

Fig. 3. Effect of combined recompression and oxygen breathing on air bubbles in rat spinal white matter. Recompression was to 284 kPa between first and second point of each curve. Bubble shrinking rate was recalculated from μm^2/min to mm^2/min. Individual symbols represent 1 bubble curve.

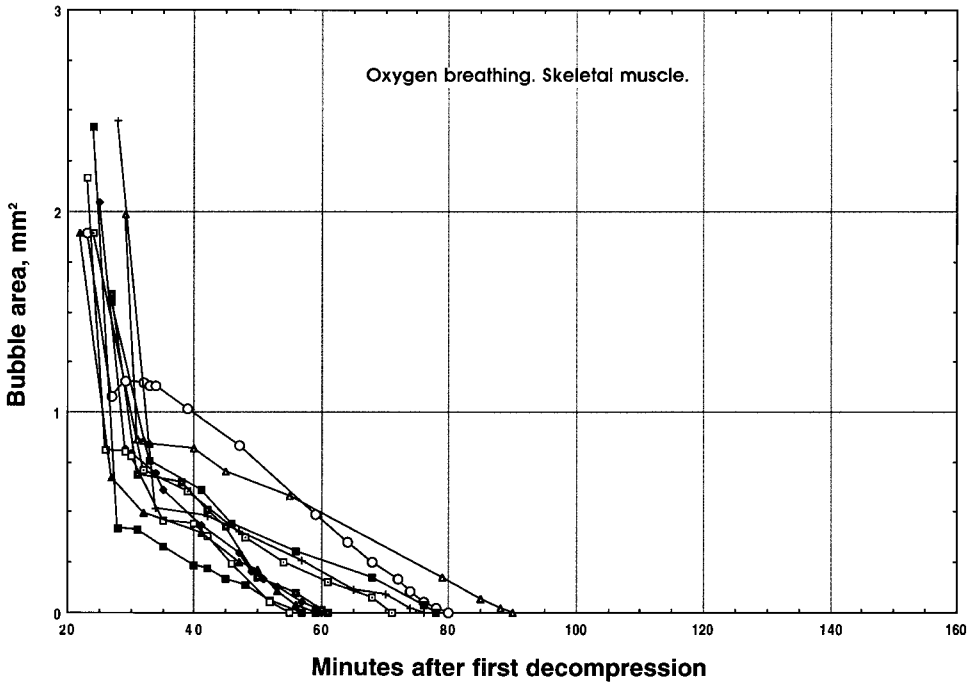

Fig. 4. Effect of combined recompression and oxygen breathing on air bubbles in rat skeletal muscle. Recompression was to 284 kPa between first and second point of each curve. Bubble shrinking rate was recalculated from μm^2/min to mm^2/min. Individual symbols represent 1 bubble curve.

For all tissues, one-way ANOVA followed by multiple comparisons between groups showed that breathing of oxygen or heliox 50:50 (at 284 kPa or 405 kPa) caused significantly faster shrinking than breathing of air ($P < 0.05$) (Table 1). Heliox 80:20 breathing caused a significantly higher shrinking rate in adipose tissue, muscle, and tendon than did air breathing. However, in spinal white matter, the higher rate during heliox 80:20, compared with air breathing, was only borderline significant at the $P < 0.05$ level ($0.1 > P > 0.05$). In spinal white matter, both heliox 50:50 breathing (i.e., at 284 and 405 kPa) and oxygen breathing proved significantly faster than heliox 80:20 breathing. There were no significant differences in the mean bubble shrinking rates between heliox 80:20, heliox 50:50, and oxygen in the adipose, muscle, and tendon tissues (Table 1).

General Condition of the Animals

During the initial pressure exposure with air breathing, the respiratory rates of the rats remained unaf-

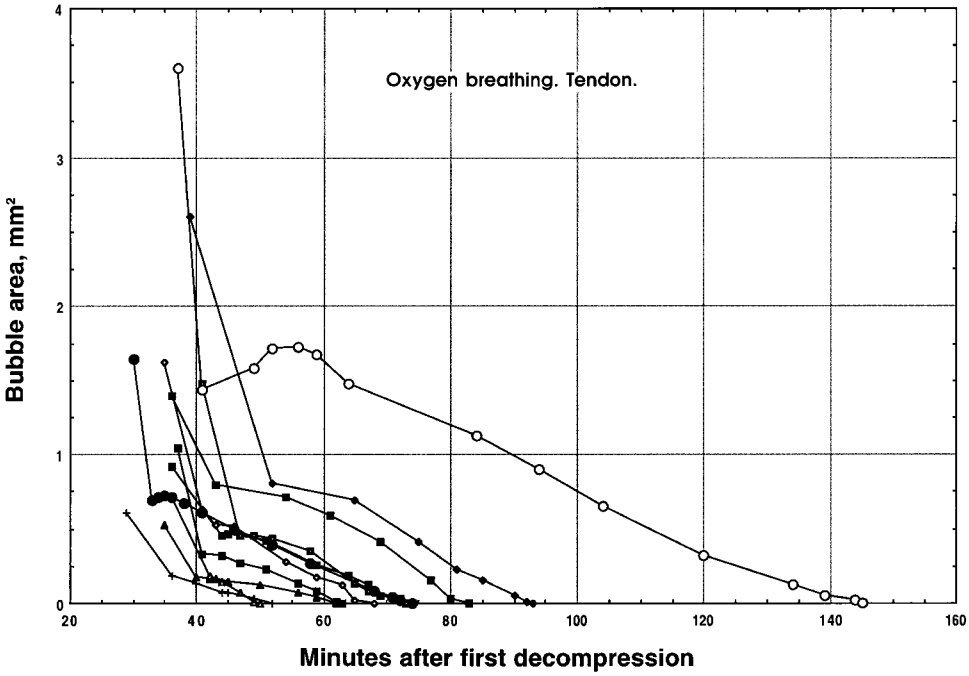

Fig. 5. Effect of combined recompression and oxygen breathing on air bubbles in rat tendon. Recompression was to 284 kPa between first and second point of each curve. Bubble shrinking rate was recalculated from μm^2/min to mm^2/min. Individual symbols represent 1 bubble curve.

Table 1. *Effects of breathing gases on air bubble shrinking rate during recompression to 284 kPa*

	Air	*n*	Oxygen	*n*	Heliox 80:20	*n*	Heliox 50:50	*n*
Adipose tissue	10.0 ± 4.8	6	29.7 ± 3.3*	4	23.5 ± 2.4*	4	27.5 ± 9.6*	4
Spinal white matter	3.6 ± 1.2	9	22.5 ± 9.8*†	6	10.9 ± 2.6‡	6	20.3 ± 12.8*†	6
Skeletal muscle	5.3 ± 1.2	4	19.5 ± 4.4*	4	21.6 ± 5.1*	4	23.3 ± 3.5*	4
Tendon	8.4 ± 1.9	5	16.6 ± 2.1*	4	19.0 ± 4.8*	4	19.3 ± 6.4*	4

Shrinking rate values are mean ± SD, calculated as ($\mu m^2 \times 10^3$)/min; *n*, number of animals. *$P < 0.05$ compared with air; †$P < 0.05$ compared with heliox 80:20; ‡$0.1 > P > 0.05$ compared with air.

fected. During decompression, their breathing rate increased transiently. This increased respiratory rate subsided during preparation of the animal and before recompression was initiated. Three rats died of decompression sickness with innumerable bubbles in their veins after the long pressure exposure (i.e., 4 h) and three after the 1-h pressure exposure.

In the surviving animals, no intra- or extravascular bubbles were observed during the microscopic examination performed after decompression from the second pressure exposure.

During the initial pressure exposures, MAP varied in most cases between 140–170 mmHg (range of 120–180 mmHg). During decompression, it fell to a level of 100–120 mmHg (range of 80–150 mmHg). When the animals were recompressed breathing either air, heliox (80:20 or 50:50), or oxygen, MAP varied over a wide range of 80–170 mmHg. In all the experiments, the vaginal temperature varied between 36.0 and 38.0°C. The tissue temperatures were in the range of 35.0–38.0°C, and in most cases 36.0–37.0°C, with a tendency toward a lower temperature in the tail tendon (35.0–37.0°C).

Adipose tissue (n = 18). In one rat, several spontaneous extravascular bubbles were observed in the adipose tissue after decompression. In all experiments, blood perfusion was clearly visible during the observation period.

Spinal white matter (n = 27). In one rat, intravascular bubbles were observed traversing the pial vessels during the preparation phase after the initial pressure exposure. During the whole observation period, circulation in the larger pial vessels was clearly visible, whereas perfusion in the smaller vessels close to the injected bubble was impeded.

Skeletal muscle (n = 16). In one rat, extravascular bubbles were observed in adipose tissue and muscle after the initial pressure exposure. During the experiments, blood perfusion was clearly visible in vessels with a diameter of 10–15 μm and seemed unaffected throughout the experiment. Occasionally, small muscle fiber twitches could be seen.

Tendon (n = 17). At all times, blood perfusion was clearly visible in the small vessels (10–15 μm diameter). When splitting the tail skin from the tendon, some bleeding was observed from the exposed skin.

The treatment groups were not statistically different (by one-way ANOVA test) with respect to mean time from decompression to time of first observation and recompression or with respect to the mean size of injected bubbles.

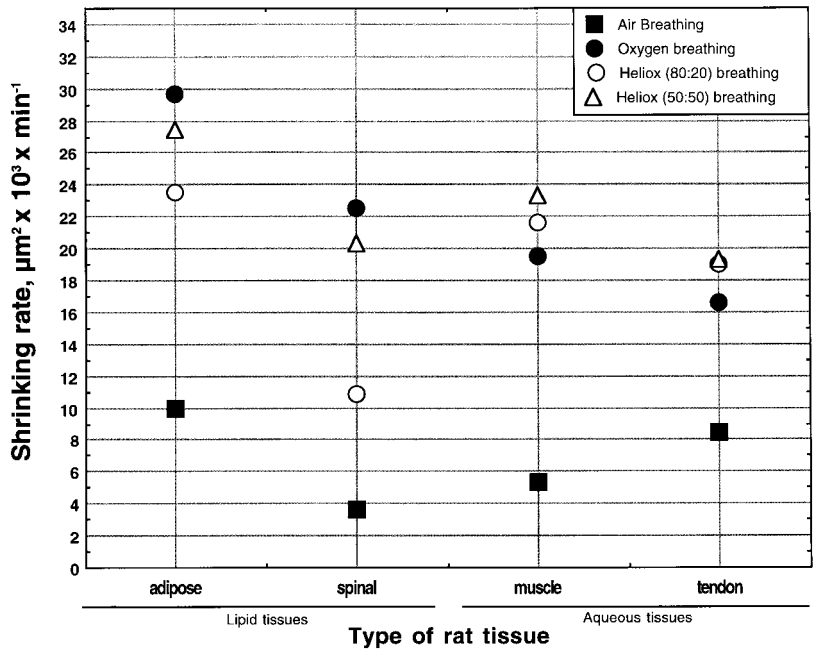

Fig. 6. Bubble shrinking rates at 284 kPa in rat tissues.

DISCUSSION

In all experiments, regardless of the tissue being studied, an initial reduction of bubble area was seen, roughly corresponding to the (re)compression according to the law of Boyle. The fate from then on depended on the breathing gas.

Air Breathing

Regardless of the tissue studied, all bubbles shrank consistently during air breathing until they disappeared from view. This is to be expected because recompression will reverse the pressure gradients for gas exchange between bubble and tissue, thus increasing the gradient forcing gas into tissue.

Oxygen Breathing

Hyldegaard and Madsen (19, 22) previously reported that air bubbles in adipose tissue may grow for up to 2 h before shrinking and disappearing during oxygen breathing when studied at both normo- and hypobaric conditions. Bubble growth during oxygen breathing was most pronounced during hypobaric conditions (22). Similarly, injected air bubbles in rat spinal white matter, tendon, and eye initially grew during oxygen breathing at normobaric conditions before they shrank and disappeared (23, 20).

When a bubble is generated by decompression or injected into a tissue, its P_{O_2} must be low, as determined by the partial pressure in the surrounding tissue (41, 45). Because oxygen is consumed metabolically and substituted by CO_2, which is highly soluble, air or nitrogen bubbles would not be expected to grow during oxygen breathing. However, in the experiments presented here, we found that oxygen breathing during recompression caused some bubbles to grow transiently before shrinking and disappearing (Figs. 2–5). This initial bubble growth indicates that the net flux of oxygen into the bubble exceeds the concomitant net flux of nitrogen out of the bubble. This unequal exchange is favored by a number of factors: *1*) the higher solubility in blood of oxygen than of nitrogen (1, 46), *2*) the oxygen carriage by hemoglobin as long as the P_{O_2} in the bubble is below 90–100 Torr, and *3*) oxygen's higher diffusibility in the tissues than of nitrogen. Obviously, it must also be influenced by *4*) the blood flow rate and *5*) the rate of oxygen consumption by the tissue, because a high ratio between oxygen delivery and oxygen consumption would favor bubble growth. Furthermore, *6*) the initial P_{O_2} is important for the oxygen diffusion gradient and may also influence the perfusion rate, and, finally, *7*) dumping of dissolved nitrogen from the surrounding tissue into the bubble as its P_{N_2} declines from dilution with oxygen may also favor growth.

As the bubble content of pure oxygen increases, the P_{O_2} gradient between blood and bubble disappears, and the bubble will shrink as oxygen diffuses to the surrounding metabolizing tissue.

Although some bubbles grew up to 1.39-fold (Fig. 2), this transient increase in bubble size during oxygen breathing under hyperbaric conditions was smaller and of much shorter duration than that observed at hypo- or normobaric conditions as described above. This could be expected because *1*) the P_{O_2} of the bubble and surrounding tissue will increase to a level at which oxygen transport with hemoglobin is of no importance (P_{O_2} = 100 Torr; arterial oxygen saturation = 1.0) faster during oxygen breathing at hyperbaric conditions than during oxygen breathing at sea level or hypobaric pressures, *2*) nitrogen in the bubble (and tissue) must disappear faster during oxygen breathing at elevated pressure because of the increased oxygen window (45). *3*) Because the gas switch occurred before recompression, part of a volume increase may be "hidden" in the initial shrinkage caused by recompression according to Boyle-Mariott's law, and *4*) the nitrogen gradient from the surrounding tissue to the bubble has been reversed by recompression. *5*) Bubble kinetic models, as well as experimental observations, suggest that the role of metabolic gases, i.e., oxygen and CO_2, and water vapor as contributors to the bubble volume during oxygen breathing may be of greater importance at hypo- and normobaric conditions compared with the hyperbaric situation (22, 43). Obviously, the relative importance of the many, partly opposing, factors in bubble evolution may vary depending on the ambient pressure.

Treatment of decompression sickness after air diving usually combines recompression and pure oxygen breathing (31, 39, 40). However, oxygen as the sole therapeutic gas has two fundamental limitations. First, the maximal therapeutic partial pressure and the acceptable duration of breathing are limited by central nervous system and pulmonary toxicity (5). Second, its diffusibility into fatty tissue is twice that of nitrogen and four times that of helium (13, 26). This may, as shown, cause a transient increase in the volume of nitrogen bubbles, especially in tissues with a low oxygen consumption rate. These findings could also explain the occasionally observed clinical phenomenon of an initial worsening of symptoms during the administration of hyperbaric oxygenation (2, 9, 26, 31). Growth of bubbles, even if limited, is obviously undesirable. However, in a damaged tissue with edema and hemorrhage, oxygen breathing has the advantages of increasing the arterial oxygen concentration and reducing edema (24) because of vasoconstriction and blood flow reduction (4, 28) and, furthermore, a reduced tendency of leukocytes to block microvessels after exposure to bubbles (47).

Heliox Breathing

During heliox 80:20 and heliox 50:50 breathing, we found that bubbles in adipose tissue and spinal white matter shrink at a rate faster than that seen during air breathing. In the present heliox 50:50 experiments, bubble growth was never observed as it was during recompression breathing oxygen. Furthermore, the rate of reduction in spinal white matter during breathing of heliox 50:50 was significantly faster than during

both air and heliox 80:20 breathing (Table 1). In case of perfusion-limited gas exchange, this difference in the rate of disappearance can be explained by the greater solubility of nitrogen than helium in blood (13, 26, 46), because this will facilitate the transport of nitrogen from the bubble to the lungs, compared with that of helium from lungs to bubble. In case of diffusion limitation, the product of the solubility coefficient and diffusion coefficient, i.e., the diffusibility, is greater for nitrogen than for helium in lipid tissues (13, 26). However, explaining bubble shrinkage after a shift from air to heliox breathing on the basis of gas solubilities in blood disregards the fact that helium and nitrogen not only will exchange between blood and bubble but also with the surrounding tissue. In lipid tissues, the tissue-blood partition coefficient for nitrogen is 2.6 times that of helium, which makes these tissues saturate (and desaturate) with helium more than twice as fast as with nitrogen. Thus a transient state of supersaturation may be created, causing growth of nitrogen bubbles during breathing of a heliox mixture as suggested by Lambertsen and Idicula (30) and D'Aoust and co-workers (6). The results of the experiments presented here are at variance with the findings of Lambertsen and Idicula (30) and D'Aoust et al. (6). However, the fact that all bubbles shrank and disappeared during heliox breathing at a rate faster than during breathing of air suggests that direct exchange of gas between bubble and the perfusing blood, under our experimental circumstances, is more important for bubble evolution than gas exchange with the surrounding tissue.

In aqueous tissues, nitrogen bubbles would be expected to grow during heliox breathing if the gas exchange between blood and bubbles is limited by extravascular diffusion because the diffusibility of helium in water is 1.4 times that of nitrogen (46). The present results, as well as our previous report (20), suggest that extravascular diffusion between bubble and blood does not limit gas exchange in muscle and tendon under the circumstances of these experiments. So far, our results are consistent with a primarily perfusion-limited gas exchange between blood and bubbles (solubilities in blood $He < N_2 < O_2$) because nitrogen disappeared faster from the bubbles than helium entered.

Previous experiments (21) using SF_6-O_2 (80:20) breathing in treatment of air bubbles in lipid and aqueous tissues suggest that countercurrent exchange may be of importance for gas exchange in some tissues. Countercurrent, a mechanism whereby gas is shunted from arteries to veins or vice versa, has been demonstrated in both skeletal muscle and brain by Sejrsen and Tønnesen (34) and in muscle by Piiper and Meyer (32) and has been discussed in relation to decompression sickness by Homer et al. (17). Recent bubble kinetic modeling studies showed that countercurrent may influence bubble evolution (14, 15, 44). Countercurrent will tend to prevent helium from reaching the bubble and maintain nitrogen in the bubble, but nitrogen should be less affected by this mechanism than helium is. Consequently, it will increase the rate of bubble shrinkage during heliox breathing.

Clinically, heliox 50:50 breathing at 405 kPa has been used with a beneficial effect in the treatment of decompression sickness (8, 10, 12, 25, 29, 36). It has two advantages compared with the standard oxygen schedule: *1*) the possibility of higher treatment pressure and *2*) using an inert gas that does not cause bubble growth. If the standard treatment table, using pure oxygen at a maximal pressure of 284 kPa, is insufficient to treat the symptoms of the diver, then recompression to higher pressures using inert gases may be necessary. Most treatment facilities will be able to raise the pressure by having the diver breathe air or nitrox. Standard mixtures of nitrox are 50:50 or 32.5:67.5 (40). In the present experiments, breathing of heliox 50:50 made bubbles disappear as fast as 100% oxygen breathing at the same pressure without any initial growth. From this data, heliox 50:50 may well be suggested as the breathing mixture of choice for the treatment of air-diving-induced decompression sickness.

The technical assistance of Senior Technician Israel Shreger is gratefully acknowledged. This work would have been impossible without it. A special thanks is given to Senior lecturer and consultant Philip B. James in assisting us with correction of English grammar and writing of the manuscript.

The project was supported by Statens Sundhedsvidenskabelige Forskningsråd (Grants 12-9160, 12-0336-1, and 12-1073-1), Fonden til Lægevidenskabens Fremme, AGA AB Medical Research Fund, Idrættens Forskningsråd, The Laerdal Foundation for Acute Medicine, and Novo Nordisk Fond.

REFERENCES

1. **Altman PL and Dittmer DS.** *Respiration and Circulation*. Bethesda, MD: Federation of American Societies for Experimental Biology, 1971.
2. **Ambriz G and Morales V.** Progressive deterioration after immediate treatment and long term sequelae of spinal embolism. A prospective clinical study of one case (Abstract). *Undersea Hyperb Med* 24: 26, 1997.
3. **Armitage PMA and Berry G.** *Statistical Methods in Medical Research*. Oxford, UK: Blackwell Scientific, 1987.
4. **Bergø GW and Tyssebotn I.** Cerebral blood flow distribution during exposure to 5 bar oxygen in awake rats. *Undersea Biomed Res* 19: 339–354, 1992.
5. **Clark JM.** *The Physiology and Medicine of Diving*. London, UK: Saunders, 1993, p. 121–170.
6. **D'Aoust BG, Smith KH, Swanson HT, and White R.** Venous gas bubbles: production by transient, deep isobaric counterdiffusion of helium against nitrogen. *Science* 197: 889–891, 1977.
7. **Douglas JDM and Robinson C.** Heliox treatment for spinal decompression sickness following air dives. *Undersea Biomed Res* 15: 315–319, 1988.
8. **Drewry A and Gormann DF.** A preliminary report on a prospective randomized double-blind controlled study of oxygen and oxygen-helium in the treatment of air-diving decompression illness (Abstract). *Undersea Hyperb Med* 20: 19, 1993.
9. **Elliott DH.** Treatment of decompression illness. *Proc Undersea Hyperb Med Soc Workshop 45th Palm Beach, FL, 1996*, p. 185–203.
10. **Goldenberg I, Shupak A, and Shoshani O.** Oxy-helium treatment for refractory neurological decompression sickness: a case report. *Aviat Space Environ Med* 67: 57–60, 1996.
11. **Goodmann MV and Workman RD.** *Minimal Recompression, Oxygen-Breathing Approach to Decompression Sickness in Divers and Aviators*. Washington, DC: Dept. of the Navy, 1965. (Navy Experimental Diving Unit Rep. 5-65)

12. **Gorman DF.** Treatment of decompression illness. *Proc Undersea Hyperb Med Soc Workshop 45th Palm Beach, FL, 1996*, p. 96–100.
13. **Hills BA.** Scientific considerations in recompression therapy. *Proc VII Eur Undersea Biomed Soc Congr Cambridge, UK, 1981*, p. 143–162.
14. **Himm JF, Albin G, Jian Y, and Homer LD.** The effects of counter-current exchange on the evolution of gas bubbles in tissue (Abstract). *Undersea Hyperb Med* 23: 71, 1996.
15. **Himm JF and Homer LD.** A model of extravascular bubble evolution: effect of changes in breathing gas composition. *J Appl Physiol* 87: 1521–1531, 1999.
16. **Hjelle JO, Molvaer OJ, Risberg J, Nyland H, and Eidsvik S.** Case report: treatment of neurological decompression illness from air diving in a heliox saturation environment (Abstract). *Proc XVII Eur Undersea Biomed Soc Congr Heraklion, Greece, 1991*, p. 299.
17. **Homer LD, Weathersby PK, and Survanshi S.** How countercurrent blood flow and uneven perfusion affect the motion of inert gas. *J Appl Physiol* 69: 162–170, 1990.
18. **Hyldegaard O, Kerem D, Madsen J, and Melamed Y.** Effect of combined recompression and air, heliox or oxygen breathing on air bubbles in rat spinal white matter. *Proc XIX Eur Undersea Baromed Soc Congr Trondheim, Norway, 1993*, p. 292–296.
19. **Hyldegaard O and Madsen J.** Influence of heliox, oxygen and N_2O-O_2 breathing on N_2 bubbles in adipose tissue. *Undersea Biomed Res* 16: 185–193, 1989.
20. **Hyldegaard O and Madsen J.** Effect of air, heliox and oxygen breathing on air bubbles in aqueous tissues in the rat. *Undersea Hyperb Med* 21: 413–424, 1994.
21. **Hyldegaard O and Madsen J.** Effect of SF_6-O_2 (80/20) breathing on air bubbles in rat tissues. *Undersea Hyperb Med* 22: 355–365, 1995.
22. **Hyldegaard O and Madsen J.** Growth of air bubbles in adipose tissue during hypobaric oxygen breathing (Abstract). *Undersea Hyperb Med* 24: 93, 1997.
23. **Hyldegaard O, Møller M, and Madsen J.** Effect of heliox, oxygen and N_2O-O_2 breathing on injected bubbles in spinal white matter. *Undersea Biomed Res* 18: 361–371, 1991.
24. **Hyldegaard O, Møller M, and Madsen J.** Protective effect of oxygen and heliox breathing on the development of spinal decompression sickness. *Undersea Hyperb Med* 21: 115–128, 1994.
25. **Imbert JP.** Treatment of decompression illness. *Proc Undersea Hyperb Med Soc Workshop 45th Palm Beach, FL, 1996*, p. 389–394.
26. **James PB.** Problem areas in the therapy of neurological decompression sickness. *Proc VII Eur Undersea Biomed Soc Congr Cambridge, UK, 1981*, p. 127–142.
27. **James PB, Imbert JP, and Arnoux GA.** *The Comex Medical Book*. Marseille, France: Companie Maritime d'Expertises, 1986.
28. **Jamieson D and Van Den Brenk HAS.** Measurement of oxygen tensions in cerebral tissue of rats exposed to high pressures of oxygen. *J Appl Physiol* 18: 869–876, 1963.
29. **Kol S and Melamed Y.** Oxy-helium treatment for spinal decompression sickness following air dives. *Undersea Hyperb Med* 20: 147–154, 1993.
30. **Lambertsen CJ and Idicula J.** A new gas lesion syndrome in man induced by "isobaric counterdiffusion." *J Appl Physiol* 39: 434–443, 1975.
31. **Moon RE and Gorman DF.** *The Physiology and Medicine of Diving*. London, UK: Saunders, 1993, p. 506–542.
32. **Piiper J and Meyer M.** Diffusion-perfusion relationships in skeletal muscle: models and experimental evidence from inert gas washout. *Adv Exp Med Biol* 169: 457–465, 1984.
33. **Rasband W.** *Image Processing and Analysis*, version 1.61. Washington DC: National Institutes of Health Research Services Branch, http://rsb.info.nih.gov/nih-image/download.html, 1996.
34. **Sejrsen P and Tønnesen KH.** Shunting by diffusion of inert gasses in skeletal muscle. *Acta Physiol Scand* 86: 82–91, 1972.
35. **Sergysels R, Jasper N, Delaunois L, Chang HK, and Martin RR.** Effect of ventilation with different gas mixtures on experimental lung air embolism. *Respir Physiol* 34: 329–343, 1978.
36. **Shupak A, Melamed Y, Ramon Y, Bentur Y, Abramovich A, and Kol S.** Helium and oxygen treatment of severe, air-diving-induced neurological decompression sickness. *Arch Neurol* 54: 305–311, 1997.
37. **SPSS.** *Statistical Package of the Social Sciences*. Chicago, IL: SPSS, 1998.
38. **Strauss RH and Kunkle TD.** Isobaric bubble growth: a consequence of altering atmospheric gas. *Science* 186: 443–444, 1974.
39. **Dept. of the Navy.** *U.S. Navy Diving Manual* (Rev. 2). Washington, DC: Dept. of the Navy, 1988, p. 1.8.1–8.72.
40. **Dept. of the Navy.** *U.S. Navy Diving Manual* (Rev. 3). Washington, DC: Best Publishing, 1996, p. 1.8.1–8.72.
41. **Van Liew HD, Bishop B, Walder D, and Rahn H.** Effects of compression on composition and absorption of tissue gas pockets. *J Appl Physiol* 7: 111–121, 1965.
42. **Van Liew HD and Burkard ME.** Computer simulation of growth and decay of decompression bubbles when breathing gas is changed (Abstract). *XXXII Internat Congr Physiol Sci Glasgow, Scotland, 1993*, p. 220.
43. **Van Liew HD and Burkard ME.** Simulation of gas bubbles in hypobaric decompressions: roles of O_2, CO_2 and H_2O. *Aviat Space Environ Med* 66: 50–55, 1995.
44. **Van Liew HD and Raychaudhuri S.** Diffusive shunting between arteries and veins: effects on washing and washout of inert gasses in tissue (Abstract). *Undersea Hyperb Med* 23: 24, 1996.
45. **Vann RD and Thalmann ED.** *The Physiology and Medicine of Diving*. London, UK: Saunders, 1993, p. 376–432.
46. **Weathersby PK and Homer LD.** Solubility of inert gasses in biological fluids and tissues: a review. *Undersea Biomed Res* 7: 277–296, 1980.
47. **Zamboni WA, Allan CR, Robert CR, Graham H, Suchy H, and Kuchan OJ.** Morphologic analysis of the microcirculation during reperfusion of ischemic skeletal muscle and the effect of hyperbaric oxygen. *Plast Reconstr Surg* 91: 1110–1123, 1993.